Adaptive Quantization in Multispectral Image Compression for Equalizing Visual Error Distribution

Yuri Murakami,[*†] Hiroyuki Manabe,[‡] Takashi Obi[‡], Masahiro Yamaguchi,[†‡] and Nagaaki Ohyama[*†]

[*] *Tokyo Institute of Technology, Frontier Collaborative Research Center, Yokohama, Japan*

[†] *Telecommunications Advancement Organization of Japan, Akasaka Natural Vision Research Center, Tokyo, Japan*

[‡] *Tokyo Institute of Technology, Imaging Science & Engineering Laboratory, Yokohama, Japan*

This article proposes an adaptive nonlinear quantization method for multispectral image compression. When linear scalar quantization is applied for multispectral image compression, extremely large error is perceived in low-luminance colors due to the nonlinear phenomenon of human vision. In the proposed method, quantization tables are switched pixel by pixel depending on the corresponding luminance. The switching rule is determined according to the relationship between the luminance and the error in the uniform color space. As a result, distribution of the error in the uniform color space can be equalized and the error in the low-luminance pixels is suppressed. Experimental results using a 16-band multispectral image of an oil painting shows the effectiveness of the proposed method.

Journal of Imaging Science and Technology 46: 507–512 (2002)

Introduction

Multispectral imaging technique is expected to be one of the promising solutions for high fidelity color image reproduction, in the applications such as tele-medicine,[1] electronic museum[2] and on-line shopping etc. Multispectral images have been used in the field of remote sensing, and compression technique has been actively investigated for their efficient transmission originated from the large capacity of multispectral images.[3–5] The compression error of multispectral images is usually measured by the difference between the original and the restored multispectral image signal. However, in the visual application, it is important to keep the error in the reconstructed color images small. There have been recently reported several researches in which the colorimetric error is evaluated. Most of them are transform-based compressions;[6–8] namely, a combination of linear transformations for inter- and intra-band decorrelation and a linear scalar quantization, though sub-sampling technique has been also introduced.[8]

As a inter-band decorrelation method, we proposed a modified version of Karhunen–Loeve transform (KLT), called weighted KLT (WKLT).[9] Applying this method to multispectral images, the colorimetric error is decreased as compared with conventional KLT. However, the perceived error in the low-luminance pixels becomes large when WKLT coefficients are linearly quantized.[9] In the visual application for high fidelity color reproduction, it is considerably important that the perceptual color difference is uniformly reduced. This article proposes a nonlinear adaptive quantization method for transform coefficients. After a brief review of WKLT, we propose adaptive quantization for WKLT coefficients. The proposed method is applied to the multispectral image of an oil painting and the results are then shown.

WKLT for Inter-Band Decorrelation

This section briefly reviews WKLT and its application to the inter-band decorrelation of multispectral images considering colorimetric error. KLT gives the optimum low-dimensional approximation of high-dimensional vector through linear transformation. To the contrary, WKLT gives the low-dimensional approximation such that the mean square error in a specific space, M'-dimensional space C, is minimum. Let $\mathbf{f}$ be an M-dimensional original vector and $\mathbf{P}$ be the $M' \times M$ projection matrix to the space C. In Ref. 9, we have demonstrated that if $\mathbf{P}^T\mathbf{P}$ becomes a diagonal matrix, denoted by $\mathbf{W}^2$, the desired approximation vector is obtained through the KLT of $\mathbf{Wf}$; we call this WKLT. According to this result, forward WKLT of $\mathbf{f}$ is expressed as

$$\alpha_j = \mathbf{v}_j{}^T \mathbf{Wf}, \tag{1}$$

where $\mathbf{v}_j$ is j-th eigenvector of the correlation matrix of $\mathbf{Wff}$ as

$$\left\langle \mathbf{Wff}^T\mathbf{W} \right\rangle \mathbf{v}_j = \omega_j \mathbf{v}_j, \tag{2}$$

and ω_j is j-th eigen value. Inverse WKLT is given by

$$\hat{\mathbf{f}}_J = \mathbf{W}^{-1} \sum_{j=1}^{J} \alpha_j \mathbf{v}_j, \tag{3}$$

Original manuscript received February 19, 2002

where $\hat{\mathbf{f}}_J$ is J-dimensional approximation of $\mathbf{f}$.

Consider that $\mathbf{f}$ is a sampled spectral reflectance and the error-evaluating space C is CIE 1931 XYZ color space under various kinds of viewing illuminations. If we can assume that the correlation of those illumination spectra is a scalar multiple of an identity, $\mathbf{P}^T\mathbf{P}$ becomes a diagonal whose (i, i) element is written by

$$[\mathbf{W}]_{i,i} = \sqrt{x_i^2 + y_i^2 + z_i^2}, \tag{4}$$

where x_i, y_i and z_i are i-th elements of sampled XYZ color matching functions, respectively. In the inter-band decorrelation, therefore, spectral reflectance is estimated from multispectral image at first, after that, the reflectance function is linearly transformed to the transform coefficients by WKLT.

Adaptive Quantization

Overview

When the WKLT coefficients are linearly quantized, the error is partially distributed in the uniform color space. To equalize the error distribution and reduce the maximum error, this article proposes a nonlinear adaptive quantization method. In this method, the fine quantization steps are applied for low-luminance pixels, so that the error in the low-luminance pixels are restrained as the same level as that of high-luminance pixels. To realize that, several quantization tables are prepared and they are switched pixel by pixel adaptively, depending on the corresponding luminance level of each pixel. To be concrete, since a pixel value is expressed by N WKLT coefficients, where N is the number of the band images, the scalar quantization is applied to them, where a quantization table corresponding to each pixel is used for every coefficient. In order to perform inverse quantization, every pixel should bring the label of its quantization table as additional information, which can be replaced by a value of a quantization step as only linear quantization is used.

Luminance Parameter

In order to decide the quantization step for a pixel, the luminance value corresponding to the pixel is required. However, the luminance depends on the viewing illuminations, for a multispectral image will be reconstructed to the colors under various viewing illuminations. To take all of them into consideration, we introduce the parameter that represents the average luminance over various viewing illuminations: luminance parameter Ψ.

As a definition of Ψ, we use

$$\Psi \equiv \sqrt{\frac{\langle Y^2 \rangle}{\langle Y_w{}^2 \rangle}}, \tag{5}$$

where Y_w is luminance of the reference white and <> is an averaging operator over the illuminations. The value,

$$\langle Y^2 \rangle,$$

can be expressed by

$$\langle Y^2 \rangle = \left\langle \left\| \mathbf{e}^T \mathbf{T}_Y \mathbf{f} \right\|^2 \right\rangle, \tag{6}$$

where $\mathbf{T}_Y$ is a diagonal matrix whose diagonal elements are sampled from a color matching function corresponding to Y, and $\mathbf{e}$ is a column vector of the spectral power distribution of illumination. Equation (6) can be rewritten as

$$\begin{aligned} \langle Y^2 \rangle &= \langle \mathbf{f}^T \mathbf{T}_Y \mathbf{e}\mathbf{e}^T \mathbf{T}_Y \mathbf{f} \rangle \\ &= \mathbf{f}^T \mathbf{T}_Y \langle \mathbf{e}\mathbf{e}^T \rangle \mathbf{T}_Y \mathbf{f} \end{aligned}. \tag{7}$$

The matrix

$$\langle \mathbf{e}\mathbf{e}^T \rangle$$

is thought to be the correlation matrix of the illumination spectra. Here, we substitute it by a scalar multiple of an identity, which means each spectrum is independent and identically distributed at each wavelength. Though real illumination spectra are usually correlated, this assumption is reasonable because the viewing illuminants have not been decided at all. Then, we have

$$\begin{aligned} \langle Y^2 \rangle &\propto \mathbf{f}^T \mathbf{T}_Y \mathbf{T}_Y \mathbf{f} \\ &= \left\| \mathbf{T}_Y \mathbf{f} \right\|^2 \end{aligned}. \tag{8}$$

Substituting this and the same for

$$\langle Y_w{}^2 \rangle$$

to Eq. (5), we have

$$\Psi = \sqrt{\frac{\left\| \mathbf{T}_Y \mathbf{f} \right\|^2}{\left\| \mathbf{T}_Y \mathbf{w} \right\|^2}}, \tag{9}$$

which can be calculated from the spectral reflectance $\mathbf{f}$ of each pixel.

Error Distribution Model

To switch the quantization steps depending on the luminance parameter Ψ, the perceptual error distribution as a function of Ψ is required. This relationship is explained by the human visual characteristics in which the luminance of the light and its perceived lightness are not linearly connected. After the review of this nonlinear relationship, the model function applied to this method is described.

There are several models representing the relationship between a luminance Y and a lightness L, one of which is the law

$$L = Y^{1/3}, \tag{10}$$

This relationship also adopted as the L^*-Y relationship in CIE 1976 L*a*b* formulas, though it is slightly modified. Taking the derivatives of Eq. (10) yields

$$\Delta L = \frac{dY^{1/3}}{dL} \Delta Y = \frac{1}{3} Y^{-\frac{2}{3}} \Delta Y. \tag{11}$$

If we regard ΔY as a quantization step and quantize Y linearly, $\Delta Y = Const. = q$, the corresponding quantization step in L, ΔL, can be represented as a function of Y as

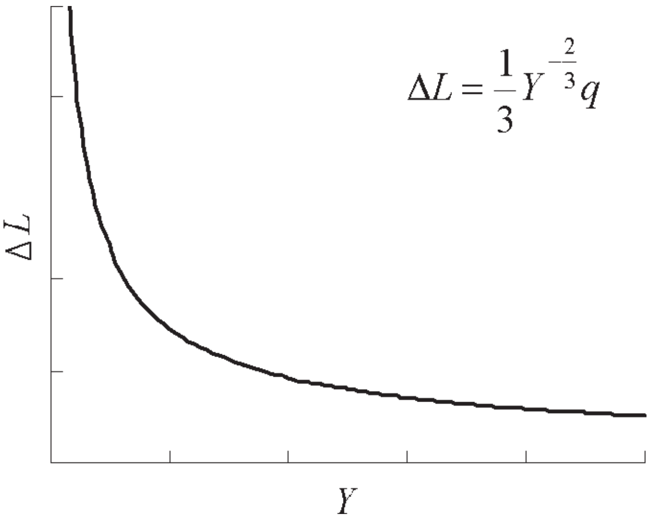

Figure 1. The nonlinear relationship between luminance Y and quantization step in lightness ΔL when Y is linearly quantized by q.

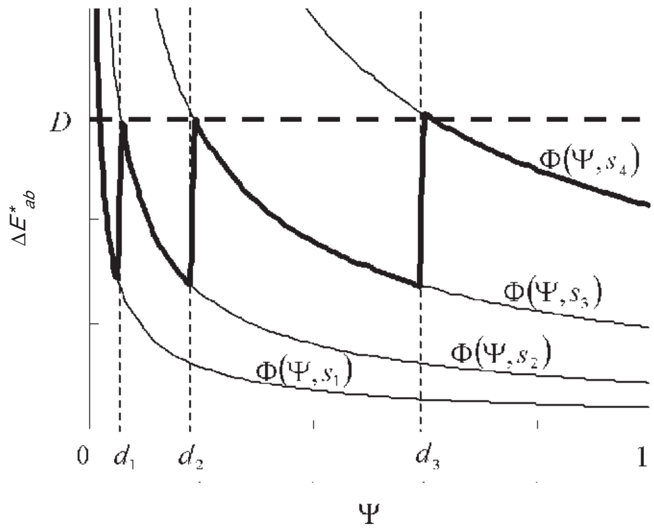

Figure 2. The schematic explanation of the classification in adaptive quantization.

$$\Delta L = \frac{1}{3} Y^{-\frac{2}{3}} q . \tag{12}$$

This relationship is depicted in Fig. 1. We can see that ΔL in the small-Y range becomes extremely large, which agrees well with the results that the perceptual errors in the low-luminance colors are much more noticeable than the other.

Based on this relationship, we define the model function of a perceptual color difference using the error in CIE 1976 L*a*b* color space. Let the notation $\Delta \overline{E}^*_{ab}(\Psi, q; k)$ be ΔE^*_{ab} averaged over all pixels with Ψ value, where q is a quantization step and k denotes the type of the viewing illumination, the model function of which is

$$\Delta \overline{E}^*_{ab}(\Psi, q; k) \propto \Phi(\Psi, q) \equiv \Psi^{-\frac{3}{2}} q , \tag{13}$$

where the factor depending on k is assumed to be a constant.

Switching Rule of Quantization Tables

The switching of the quantization steps is carried out based on the error distribution model of Eq. (13). Figure 2 is a schematic explanation of the switching, taking an example for four kinds of quantization steps s_i, i=1,..,4. Error distributions corresponding to four kinds of quantization steps are depicted as four solid curves by $\Phi(\Psi, s_i)$, i = 1,..,4. We introduce a parameter D that defines the maximum error, the level of which is indicated as a horizontal bold dotted line. The switching points d_i, i=1,…,3, are decided as the intersection points between those curves and the line of D; the points that satisfy $\Phi(d_i, s_{i+1}) = D$. Then, the pixel with the luminance parameter Ψ', where $d_{i-1} < \Psi', \leq d_i$, is quantized by the step s_i. As a result, the distribution of the error becomes the bold line in Fig. 2. If we adopt the increment rule of the quantization steps, $s_{i+1} = A s_i$, which means a relation of $\Phi(\Psi, s_{i+1}) = \Phi(\Psi, A s_i) = A\Phi(\Psi, s_i)$, the error can be restrained between D and D/A over all range of Ψ.

Finally let us consider the number of the quantization steps. As we can see in Fig. 2, the more the kinds of the steps are, the more the error distribution is equalized. However, in adaptive quantization, every pixel should bring the information of its own quantization step. The increase of the kinds of the quantization steps also brings the increase of the amount of additional information. If we use K different quantization steps for N band multispectral image, the additional information in bits per pixel (bpp) becomes $(\log_2 K)/N$, which only implies the tendency that large K can be used when N is also large. Then, the optimal K should be decided empirically considering the trade-off between the reduction of the error by adaptive quantization and the increase of the additional information.

Experiments

Flow of Experiments

The multispectral image used in the experiments is composed of sixteen bands, each of which consists of 936 × 728 pixels having 8 bits gray-level dynamic resolution. It is captured by multispectral camera (Olympus Opt. Co., Ltd.), where the central wavelength of the filters are 390, 420, 450, 480, 500, 520, 540, 560, 580, 600, 620, 640, 660, 690, 720 and 750 nm. The subject is an oil painting, and Fig. 3 shows a band image whose central wavelength is 520 nm. The schematic diagram of the experiments is shown in Fig. 4. The spectral reflectance is obtained by Wiener estimation pixel by pixel using the correlation matrix of a first-order stationary Markov sequences (ρ = 0.99). The color images are calculated from the estimated reflectance assuming viewing illuminants CIE A, D65 and F1, and these images are considered to be the original reproduced images. The WKLT bases are calculated from the estimated spectral reflectances of all pixels, and the transform coefficients are obtained by WKLT of the reflectance for each pixel. The WKLT coefficients are quantized linearly (notated LQ in the results) or adaptively (AQ). In the adaptive quantization, the number of the quantization steps is 4, where $s_{i+1} = 2s_i$, and the additional information for quantization step label becomes 0.125[bpp]. Predictive coding using one neighboring pixel is applied to the

Figure 3. A band image of the multispectral image used in the experiments. The central wavelength of the corresponding color filter is 520nm.

quantized data for intra-band decorrelation. The entropy of the resulted data is calculated for the evaluation of compression performance as

$$-\sum_{j=1}^{N}\left(\sum_{i=1}^{B_j} p_{ij}\log_2 p_{ij}\right), \qquad (14)$$

where p_{ij}, i=1,...,B_j, is the probabilities of the i-th symbols calculated from j-th WKLT coefficients and B_j is the number of the possible independent symbols. In case of adaptive quantization, the entropy of the additional information required for quantization step label is added. Coded data are decompressed and the color is calculated assuming viewing illuminants A, D65 and F1. To measure the compression error in the uniform color space, the difference between restored color images and original reproduced color images are calculated in L*a*b* color space. Various compression-rate results are obtained by changing the quantization steps.

Results

Figure 5 shows the fitness of the error distribution model defined by Eq. (13). The error ΔE^*_{ab} under D65 illuminant of each pixel is calculated in case of LQ with three kinds of quantization steps. The average error of each pixel is plotted for 20 levels of the luminance parameter Ψ. As shown in Fig. 5, the experimental data can be well approximated by the model function. At the same time, we can see that the error in the small-Ψ range becomes extremely large as it would be expected, which causes the considerably large maximum error.

Figure 6 shows the effect of equalizing error distribution by introducing AQ. The height of each bar indicates the average ΔE^*_{ab} under D65 illuminant of the pixels of corresponding Ψ value. Each quantization step is decided so that the entropy of the compressed data are equal to about 30. The symbols connected by the line indicate the frequency of the pixels of corresponding Ψ value. In this graph, we confirm that the errors by AQ in the low-Ψ range become much lower than the LQ case.

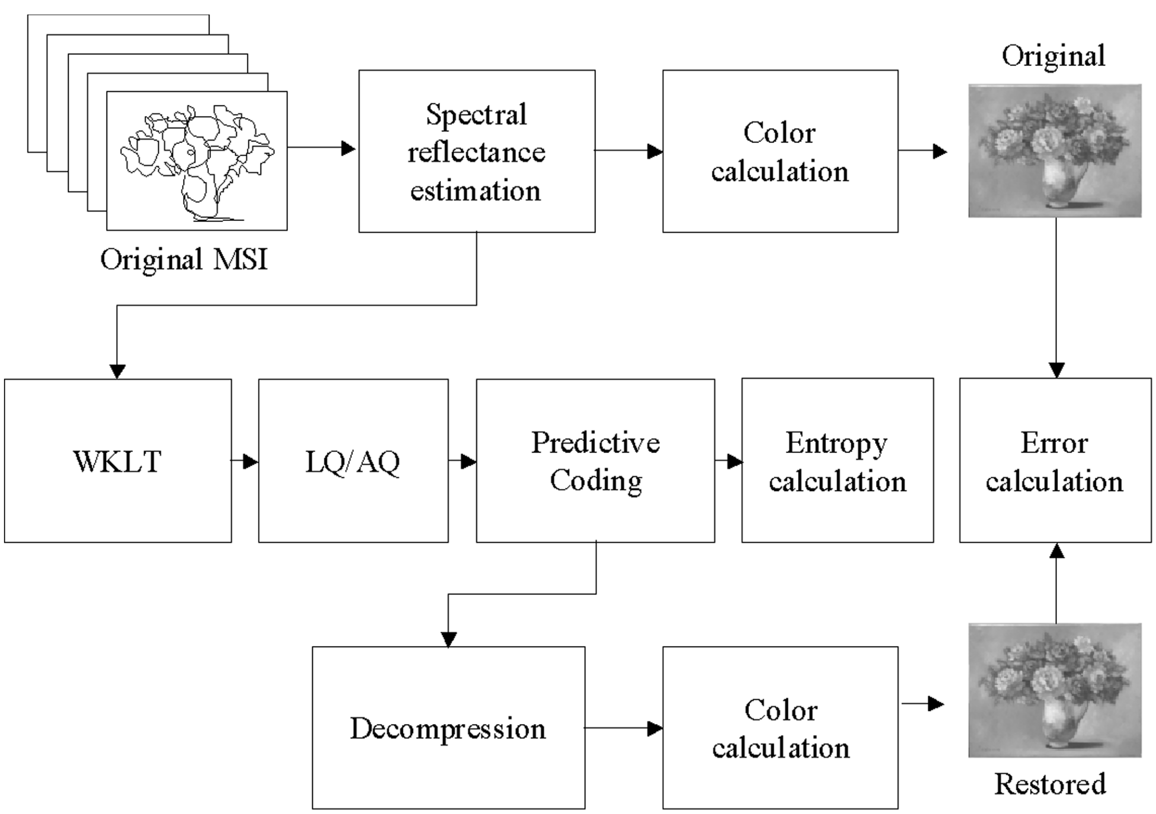

Figure 4. Flow of the experiments.

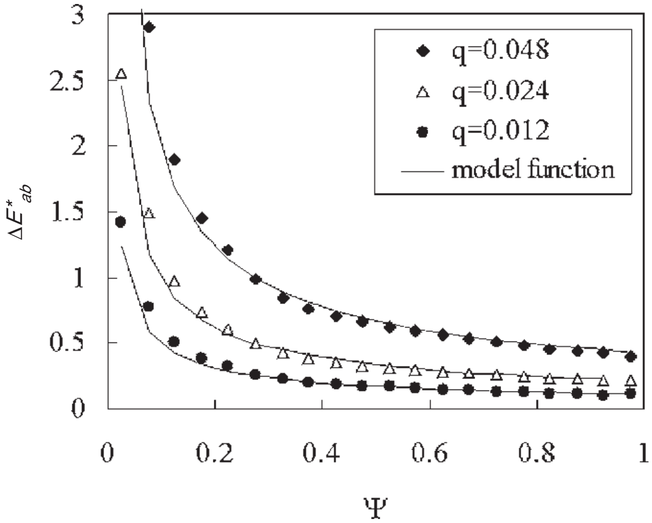

Figure 5. Certification of the model function for the error distribution.

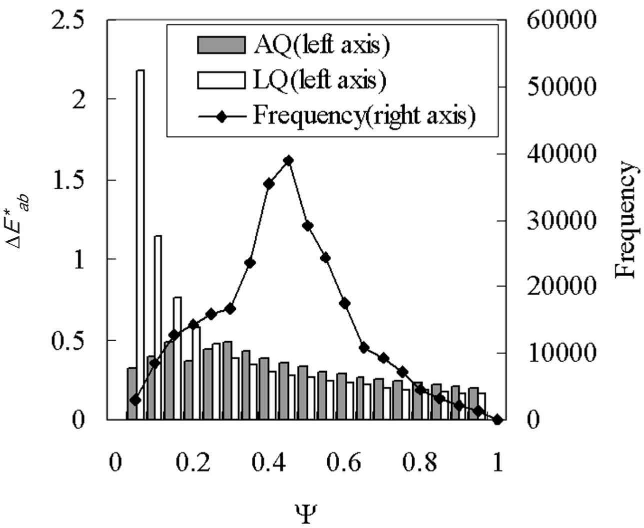

Figure 6. Effect on the equalization of the error distribution of adaptive quantization. The left axis indicates the ΔE^*_{ab} under D65 and the right axis indicates the frequency of the pixels.

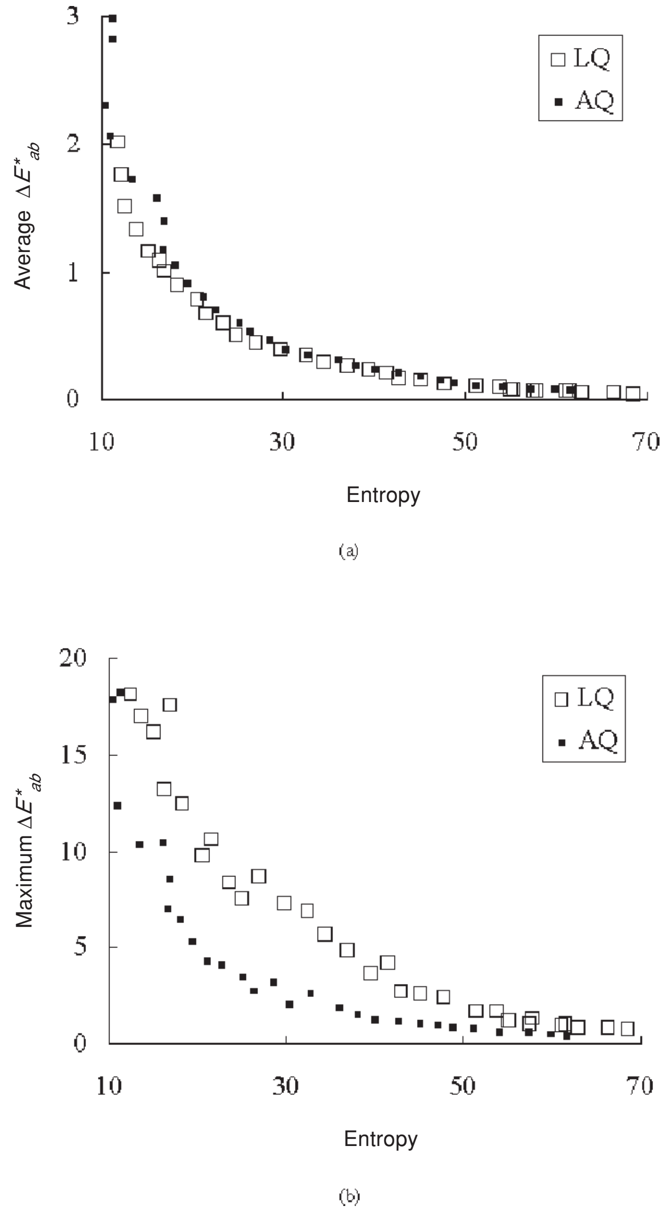

Figure 7. Comparison between LQ and AQ; (a) average and (b) maximum ΔE^*_{ab} under D65 versus the entropy.

On the contrary, in the high-Ψ range, we can see that the errors of AQ become slightly larger than LQ. It is because the bit of those pixels is somewhat assigned to the low-Ψ pixels for equalizing the error in AQ. The increase of the error in high-Ψ range depends on the distribution of the frequency of the pixels. If the frequency corresponding low-Ψ value is high, the increase of the error becomes large because the required bits assigned to those pixels becomes large also. However, in case of the distribution as shown in Fig. 6, the error in high-Ψ range is hold at a small increase.

Figure 7 shows the comparison between the compression performance of LQ and AQ. Though the average ΔE^*_{ab} of AQ becomes slightly larger comparing to LQ, the maximum error is greatly reduced over wide range of entropy.

Table I shows the average and maximum ΔE^*_{ab} of the multispectral image compressed to about 1/2 and 1/4; 1/2 corresponds about 64[bpp] and 1/4 corresponds about 32[bpp] where original data is 128[bpp]. Exact entropy values are presented in parentheses. The viewing illuminants are D65, A, F1. From these results, we can see that AQ has an effect reducing the maximum error up to about half, while the average error is not improved. This tendency can be seen at every viewing illuminant.

Conclusions

Nonlinear adaptive quantization method in multispectral image compression for high fidelity color reproduction is proposed. The switching of the quantization steps is carried out based on the error distribution model, which is derived from the luminance-lightness relation. Through the experiments using a 16-band multispectral image, we confirm that adaptive quantization equalizes the error distribution in the uniform

TABLE I. Average and Maximum ΔE^*_{ab} of the Compressed Multispectral Image to About 1/2 and 1/4.

Illumination	Average/Maximum ΔE^*_{ab} 1/2 LQ	1/2 AQ	1/4 LQ	1/4 AQ
(Entropy)	(63.16)	(63.06)	(32.32)	(32.39)
D65	0.057/1.00	0.064/0.40	0.35/5.15	0.35/2.43
A	0.061/1.22	0.067/0.45	0.36/6.38	0.35/2.31
F1	0.055/0.80	0.061/0.43	0.33/5.16	0.34/2.91

color space and reduces the maximum error to about half, and, at the same time, causes almost no increase in the average error comparing to the linear quantization result.

References

1. Y. Ohya, T. Obi, M. Yamaguchi, N. Ohyama and Y. Komiya, Natural color reproduction of human skin for telemedicine, in *Proc. SPIE Medical Imaging*, **3335**, 263–270 (1998).
2. H. Haneishi, T. Hasegawa, A. Hosoi, Y. Yokoyama, N. Tsumura and Y. Miyake, System design for accurately estimating spectral reflectance of art paintings, *Appl. Opt.* **39**, 6621 (2000).
3. T. M. Chen, D. H. Staelin and R. B. Arps, Information content analysis of Landsat image data for compression, *IEEE Trans. Geosci. Remote Sensing* **25**, 499 (1987).
4. S. Gupta and A. Gersho, Feature predictive vector quantization of multispectral images, *IEEE Trans. Geosci. Remote Sensing* **30**, 491 (1992).
5. J. A. Saghri, A. G. Tescher and J. T. Reagan, Three-dimensional transform coding of multispectral data, in *Proc. IEEE 27th Asilomar Conf. Signals, Systems & Computers*, IEEE Computer Society Press, Pacific Grove, CA, 1993, pp. 1342–1346.
6. W. Kondou, K. Miyata, H. Haneishi, and Y. Miyake, An evaluation of image quality for compressed multi-spectral image, in *Proc. Int'l Symposium on Multispectral Imaging and Color Reproduction for Digital Archives*, Chiba University, Chiba, Japan, 1999, pp. 143–146.
7. J. Parkkinen, M. Hauta-Kasari, A. Kaarna, J. Lehtonen, P. Koponen, and T Jaaskelainen, Multispectral image compression, in *Proc. 2nd Int'l Symposium on Multispectral Imaging and High Accurate Color Reproduction,* Chiba University, Chiba, Japan, 2000, pp. 49–58.
8. L. MacDonald, S. Westland and D. Liu, Multispectral Image Encoding and Compression, in *Proc. 9th Color Imaging Conference*, IS&T, Springfield, VA, 2001, pp. 135–140.
9. Yuri Murakami, Hiroyuki Manabe, Takashi Obi, Masahiro Yamaguchi and Nagaaki Ohyama, Weighted KL transform in multispectral image compression for high fidelity color reproduction, submitted to *J. Opt. Soc. Amer. A*.